

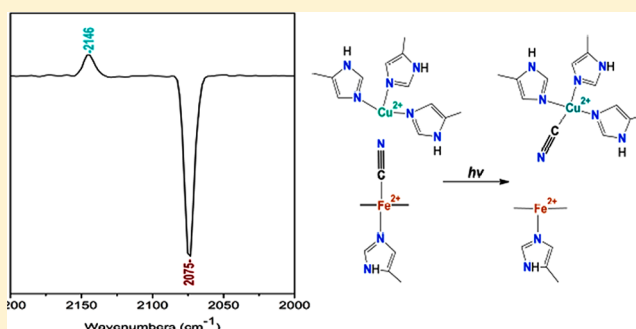
# Observation of Ligand Transfer in $ba_3$ Oxidase from *Thermus thermophilus*: Simultaneous FTIR Detection of Photolabile Heme $a_3^{2+}$ -CN and Transient $Cu_B^{2+}$ -CN Complexes

Andreas Loullis,<sup>†</sup> Mohamed Radzi Noor,<sup>‡</sup> Tewfik Soulimane,<sup>‡</sup> and Eftychia Pinakoulaki<sup>†,\*</sup>

<sup>†</sup>Department of Chemistry, University of Cyprus, P.O. Box 20537, 1678 Nicosia, Cyprus

<sup>‡</sup>Chemical and Environmental Sciences Department and Materials & Surface Science Institute, University of Limerick, Limerick, Ireland

**ABSTRACT:** FTIR and light-minus-dark FTIR spectroscopy have been employed to investigate the reaction of oxidized and fully reduced  $ba_3$  oxidase with cyanide. The characterization of the structures of the bound  $CN^-$  in the binuclear heme Fe- $Cu_B$  center is essential, given that a central issue in the function of  $ba_3$  oxidase is the extent to which the partially reduced substrates interact with the two metals. In the reaction of oxidized  $ba_3$  oxidase with cyanide the initially formed heme  $a_3^{3+}$ - $C\equiv N$ - $Cu_B^{2+}$  species with  $\nu(CN)$  frequency at  $2152\text{ cm}^{-1}$  was replaced by a photolabile complex with a frequency at  $2075\text{ cm}^{-1}$  characteristic of heme  $a_3^{2+}$ - $CN^-$ . Photolysis of the heme  $a_3^{2+}$ - $CN^-$  adduct produced a band at  $2146\text{ cm}^{-1}$  attributed to the formation of a transient  $Cu_B^{2+}$ - $CN^-$  complex. All forms are pH independent between pH 5.5–9.5 and at pD 7.5 indicating the absence of ionizable groups that influence the properties of the cyanide complexes. In contrast to previous reports, our results show that  $CN^-$  does not bind simultaneously to both heme  $a_3^{2+}$  and  $Cu_B^{2+}$  to form the mixed valence  $a_3^{2+}$ - $CN$ - $Cu_B^{2+}$  species. The photolysis products of the heme  $a_3^{2+}$ - $CN^-$ / $Cu_B^{2+}$  and heme  $a_3^{2+}$ - $CN^-$ / $Cu_B^{1+}$  species are different suggesting that relaxation dynamics in the binuclear center following ligand photodissociation are dependent on the oxidation state of  $Cu_B$ .



## INTRODUCTION

Cytochrome  $ba_3$  oxidase is a member of a superfamily of proton translocating proteins called terminal oxidases that contain a binuclear catalytic site in which the binding of exogenous ligands such as  $O_2$ ,  $CO$ , and  $NO$  and their reactions take place.<sup>1–5</sup> The enzyme has four redox centers; a mixed-valence [ $Cu_A^{1.5+}$ - $Cu_A^{1.5+}$ ] homodinuclear copper complex, a low spin heme  $b$ , and a heme  $a_3$ - $Cu_B$  binuclear site. The  $a$ -type heme contains a hydroxyethylgeranylgeranyl side chain instead of a hydroxyethylfarnesyl side chain as seen in most bacterial and eukaryotic  $aa_3$  oxidases.<sup>2</sup> Recently, it was postulated that heme-copper oxidases and  $NO$  reductases may have evolved from a common ancestor and support a possible coevolution of aerobic respiration and denitrification.<sup>3</sup> It has been reported that  $Cu_B$  in  $ba_3$  oxidase has a relative high affinity for  $CO$  ( $K_1 > 10^4$ ), in contrast to bovine  $aa_3$  oxidase, indicating unusual kinetics of electron transfer and ligand binding.<sup>4,5</sup> The kinetic properties of  $CO$  and  $CN^-$  binding were interpreted prior to the determination of the three-dimensional structure of the enzyme, and were ascribed to peculiar features in the binuclear center.<sup>5</sup> The subsequent analysis of crystal structures, however, did not reveal the presence of any characteristic features.<sup>2</sup> A full elucidation of the structure and the electron configuration of various intermediates is of profound importance for

understanding the mechanism by which the enzymes perform ligand transfer and bond formation.

Structural information of the  $O_2$ -binding binuclear center of  $ba_3$  oxidase and in cytochrome  $c$  oxidase ( $CcO$ ) superfamily have been determined from a great number of spectroscopic and computational studies of the  $CO^-$ ,  $CN^-$ , and  $NO$ -bound adducts.<sup>6–32</sup> In general,  $CO$  binds to the ferrous ( $Fe^{2+}$ ) form of heme  $a_3$ , whereas  $CN^-$  and  $NO$  bind to both oxidized ( $Fe^{3+}$ ) and reduced ( $Fe^{2+}$ ) forms of heme  $a_3$ . Because of the unusual ligand-binding kinetic properties of its binuclear center, cytochrome  $ba_3$  from *T. thermophilus* is unique among the heme-copper oxidases in being susceptible to a detailed analysis of its ligation dynamics in the heme  $a_3$ - $Cu_B$  site.<sup>3–5</sup> Resonance Raman (RR), electron nuclear double resonance (ENDOR), and electron paramagnetic resonance (EPR) spectroscopies, in conjunction with the permutations of  $^{13}C$ - and  $^{15}N$ -labeled cyanide have indicated that the reaction of oxidized  $ba_3$  with cyanide yields a heme  $a_3(II)$ - $CN$ - $Cu_B(II)$ - $CN$  complex.<sup>18–20</sup> It has been demonstrated that cytochrome  $ba_3$  reacts slowly with excess  $HCN$  at pH 7.4 to create a form of the enzyme in which  $Cu_A$ , heme  $b$ , and  $Cu_B$  remain oxidized, while heme  $a_3$  is

Received: May 25, 2012

Revised: July 3, 2012

Published: July 5, 2012

reduced by one electron, presumably with the formation of cyanogen.<sup>18</sup> The results supported a model in which one CN<sup>−</sup> binds through the carbon atom to ferrous heme *a*<sub>3</sub>, supporting a low-spin (*S* = 0) configuration on the Fe; bridging by this cyanide to the Cu<sub>B</sub> is weak or absent. Four <sup>14</sup>N atoms, presumably donated by histidine residues of the protein, provide a strong equatorial ligand field about Cu<sub>B</sub> and a second CN<sup>−</sup> is coordinated through the carbon atom to Cu<sub>B</sub> in an axial position. Although the Fe–CN modes were detected by RR spectroscopy in all of the CN-adducts, the corresponding Cu<sub>B</sub>–CN modes were not observed.<sup>18–20</sup>

The vibrational modes of cyanide when bound to heme-copper oxidases in various oxidation states have been studied by FTIR and RR spectroscopies.<sup>24–32</sup> In the oxidized form of the enzyme cyanide binds to the binuclear center to form a Fe<sup>3+</sup>–C≡N–Cu<sub>B</sub><sup>2+</sup> complex in all heme-copper oxidases studied with the exception of the reports on *ba*<sub>3</sub> oxidase.<sup>18–20,25,26,28,29</sup> There are some differences and conflicting reports on the fully reduced-CN complexes. In the bovine enzyme, modes at 2058 and 2045 cm<sup>−1</sup> have been reported; in the partially reduced enzyme the modes at 2131 and 2093 cm<sup>−1</sup> have been attributed to redox changes of the heme Fe–Cu<sub>B</sub> center or to protonation differences.<sup>25,26</sup> Of note, is the report of the modes observed at high CN<sup>−</sup> concentrations at 2093 and 2037 cm<sup>−1</sup> assigned to the binding of a second CN<sup>−</sup> to Cu<sub>B</sub>.<sup>26</sup> There are also some intriguing data regarding the properties of CN<sup>−</sup> binding to the binuclear center of *bo*<sub>3</sub> quinol oxidase and *ba*<sub>3</sub> CcO. Cytochromes *ba*<sub>3</sub> and *bo*<sub>3</sub> have notably different electron donating substrates (water-soluble cytochrome *c* versus membrane-soluble ubiquinol); however, both enzymes have the ability to catalyze dioxygen and nitric oxide reduction.<sup>3,33</sup> In a report on the FTIR spectrum of the fully reduced cyanide-bound cytochrome *bo*<sub>3</sub>, the  $\nu(\text{CN})$  was observed at 2035 cm<sup>−1</sup>.<sup>28</sup> This mode, with a frequency of 23 cm<sup>−1</sup> lower than the reported value for the corresponding frequency of bovine CcO, was interpreted to arise from the specific character of the cyanide binding to the binuclear center of cytochrome *bo*<sub>3</sub>. The shift of the C–N(Fe) mode located at 2058 cm<sup>−1</sup> in heme *a*<sub>3</sub><sup>2+</sup> to 2035 cm<sup>−1</sup> in heme *o*<sub>3</sub><sup>2+</sup> suggests a significant difference in the structure of the His-heme *a*<sub>3</sub><sup>2+</sup>/Cu<sub>B</sub><sup>1+</sup> and His-heme *o*<sub>3</sub><sup>2+</sup>/Cu<sub>B</sub><sup>1+</sup> binuclear pockets upon CN<sup>−</sup> binding. RR studies of the CN-bound complexes of heme-copper oxidases revealed significant differences between the isotope-sensitive modes of the heme Fe–CN complexes.<sup>20,27,30</sup> On this line, the reported  $\nu(\text{Fe}^{2+}\text{–CN})$  and  $\delta(\text{Fe–C–N})$  of the *aa*<sub>3</sub> oxidases at 468 and 500 cm<sup>−1</sup>, respectively, and for *bo*<sub>3</sub> for the stretching frequency at 468 and bending at 491 cm<sup>−1</sup> differ significantly from the corresponding modes reported for the *ba*<sub>3</sub> oxidase at 512 and 485 cm<sup>−1</sup>. Importantly, it has been demonstrated that in *ba*<sub>3</sub> oxidase the Fe–C–N adopts a linear geometry in which the stretching vibration appears at a higher frequency than the bending vibration.<sup>19</sup>

In the work reported here, we have examined the FTIR and light-minus-dark difference FTIR spectra of the reactions of the fully oxidized and fully reduced *ba*<sub>3</sub> oxidase with cyanide and compared the vibrational characteristics of the CN adducts with those previously reported for the *aa*<sub>3</sub> and *bo*<sub>3</sub>-type heme-copper oxidases. Upon addition of cyanide to the oxidized enzyme the heme *a*<sub>3</sub><sup>3+</sup>·C≡N–Cu<sub>B</sub><sup>2+</sup> complex was observed, and replaced by a photolabile heme *a*<sub>3</sub><sup>2+</sup>·CN<sup>−</sup> species. Photolysis of the heme *a*<sub>3</sub><sup>2+</sup>·CN<sup>−</sup> complex produced a transient Cu<sub>B</sub><sup>2+</sup>–CN<sup>−</sup> species. With the detection of the transients heme *a*<sub>3</sub><sup>2+</sup>/Cu<sub>B</sub><sup>2+</sup>–CN<sup>−</sup> and heme *a*<sub>3</sub><sup>2+</sup>/Cu<sub>B</sub><sup>1+</sup>–CO species, the mixed valence and

reduced forms of the binuclear center in *ba*<sub>3</sub> oxidase have been characterized. The reaction of *ba*<sub>3</sub> oxidase with cyanide is compared with the analogous reaction with NO where the hyponitrite intermediate was detected recently.<sup>12</sup>

## ■ EXPERIMENTAL METHODS

Cytochrome *ba*<sub>3</sub> was isolated from *T. thermophilus* HB8 cells according to the previously published procedures.<sup>2</sup> The samples used for the FTIR measurements had an enzyme concentration of ~1 mM and were placed in a desired buffer (pH 5.5, MES; pH 7.5–9.5, Tris). The pD of solutions prepared in D<sub>2</sub>O buffers was measured by using a pH meter and calculated by assuming pD = pH (observed) + 0.4. The cyanide adducts of oxidized *ba*<sub>3</sub> oxidase were prepared by the addition of buffered potassium cyanide solutions to a final concentration of ~20 mM to the protein. The fully reduced *ba*<sub>3</sub>–CN adducts were prepared under anaerobic conditions by the addition of buffered potassium cyanide solutions to a final concentration of ~10 mM to dithionite-reduced protein. Dithionite-reduced samples were exposed to 1 atm CO (1 mM) in an anaerobic cell to prepare the carbonmonoxy adduct and transferred to a tightly sealed FTIR cell under anaerobic conditions. CO gas was obtained from Linde and isotopic CN was purchased from Aldrich. The static FTIR spectra were recorded with 4 cm<sup>−1</sup> spectral resolution on a Bruker Vertex 70 FTIR spectrometer equipped with a liquid nitrogen cooled mercury cadmium telluride (MCT) detector, using the buffer as background. The contribution of HCN was removed from the spectra by subtracting the spectrum of the free ligand. A 447 nm continuous wave (c.w.) laser diode (Coherent, Cube) was used as a pump beam to photolyze the heme Fe<sup>2+</sup>–CN complex, and 30–50 difference spectra of 100 scans each (light-minus-dark) were recorded and averaged. Typically, 100 scans were averaged to provide the dark background, and then recording started 1 s after initiating sample illumination to obtain the light-minus-dark FTIR difference spectrum. Dark/light cycles were repeated with 2 s intervals. The power incident on the sample was 30 mW. With this excitation wavelength, photolysis yields of 30% and 5% were achieved for the oxidized *ba*<sub>3</sub>–CN and fully reduced *ba*<sub>3</sub>–CN complexes, respectively. Optical absorption spectra were recorded with a Shimadzu UV-1700 UV–visible spectrometer. The optical absorption spectra were also recorded before and after the FTIR measurements to ensure the formation and stability of the CN<sup>−</sup> adducts.

## ■ RESULTS

The optical absorption spectrum of oxidized *ba*<sub>3</sub> oxidase shown in Figure 1, panel a, trace A, displays a Soret maximum at 414 nm and visible maxima at 535, 562, and 660 nm. The optical spectrum of the oxidized *ba*<sub>3</sub>–CN complex shown in Figure 1, panel a, trace B, displays Soret maxima at 414 and 439 nm and visible maxima at 538 and 590 nm. The optical absorption spectrum of dithionite reduced *ba*<sub>3</sub> shown in Figure 1 panel b, trace A, displays Soret maxima at 426 (heme *b*<sup>2+</sup>) and 442 (heme *a*<sub>3</sub><sup>2+</sup>) nm and visible maxima at 530/559 (heme *b*<sup>2+</sup>) and 612 (heme *a*<sub>3</sub><sup>2+</sup>) nm. The reduced-CN complex shown in Figure 1, panel b, trace B displays Soret maxima at 426 and 440 nm and visible maxima at 530, 559, and 591 nm. The bands observed at 439/590 nm in the reaction of oxidized *ba*<sub>3</sub> oxidase with cyanide and at 440/591 nm in the reaction of fully reduced *ba*<sub>3</sub> with CN indicate the formation of a six-coordinate

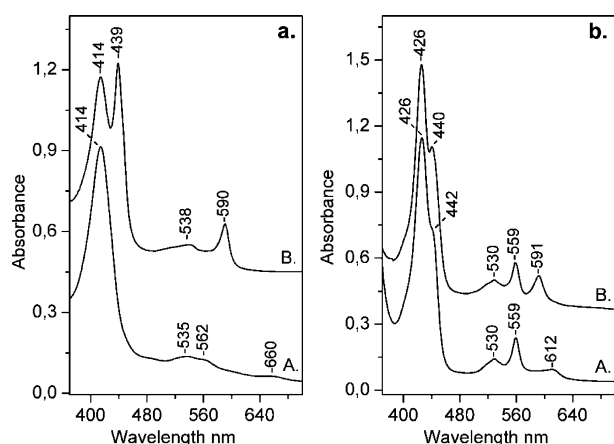


**Figure 1.** (Panel a) Optical absorption spectra of oxidized cytochrome  $ba_3$  (trace A) and of the reaction of oxidized cytochrome  $ba_3$  with cyanide (trace B) at pH 7.5. (Panel b) Optical absorption spectra of fully reduced cytochrome  $ba_3$  (trace A) and of the reaction of fully reduced cytochrome  $ba_3$  with cyanide (trace B) at pH 7.5.

low spin heme  $a_3^{2+}$ -CN $^-$  species in agreement with previous reports.<sup>18</sup>

Figure 2 shows the time-evolution of the FTIR spectra (traces A–E) of the reaction of oxidized cytochrome  $ba_3$  with

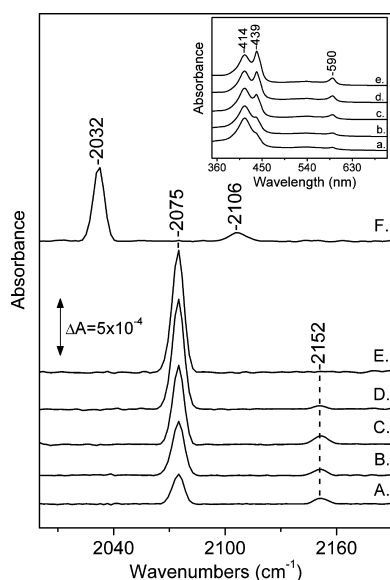


**Figure 2.** FTIR spectra of the reaction of oxidized cytochrome  $ba_3$  with  $^{12}\text{C}^{14}\text{N}$  at pH 7.5 demonstrating the time-evolution of the reaction (traces A–E). Traces A–E were obtained at 2, 4, 8, 18, and 24 h subsequent to CN $^-$  addition to the oxidized enzyme. Trace F is the spectrum of the reaction of oxidized cytochrome  $ba_3$  with  $^{13}\text{C}^{14}\text{N}$ . The inset includes the corresponding in time optical absorption spectra (traces a–e).

cyanide at the indicated times and at pH 7.5. The inset depicts the corresponding optical absorption spectra. Spectrum F is the analogous spectrum obtained at 8 h after  $^{13}\text{C}^{14}\text{N}$  addition. The bands at 2152 and 2075  $\text{cm}^{-1}$  that are present in spectra A–D shift to 2106 and 2032  $\text{cm}^{-1}$  (trace F), respectively, as cyanide mass is increased. The frequency and isotopic shift of the 2152  $\text{cm}^{-1}$  vibration are very similar to that observed and assigned to a bridging heme  $\text{Fe}^{3+}$ -C $\equiv$ N-Cu $_B^{2+}$  structure in the majority of heme-copper oxidases,<sup>24–26</sup> indicating the formation of an

analogous bridging  $a_3^{3+}$ -C $\equiv$ N-Cu $_B^{2+}$  structure in  $ba_3$  oxidase. The intensity of the 2152  $\text{cm}^{-1}$  band is weak relative to the second band observed at 2075  $\text{cm}^{-1}$  and disappears at latter times (trace E). The frequency of the latter mode and its isotopic shift allow us to assign it to the C–N stretching vibration of the CN $^-$  bound to heme  $a_3^{2+}$ , in agreement with previous resonance Raman (RR) studies that reported the  $\nu(\text{Fe}^{2+}$ -CN) and  $\delta(\text{Fe}^{2+}$ -C–N) in the reaction of cyanide with the oxidized enzyme demonstrating the reduction of heme  $a_3$ .<sup>18–20</sup> However, previous experiments have failed to detect the initially formed bridging heme  $a_3^{3+}$ -C $\equiv$ N-Cu $_B^{2+}$  structure in  $ba_3$  oxidase.

Figure 3 shows the FTIR spectra of the reaction of oxidized  $ba_3$  oxidase with cyanide in the pH 5.5–9.5 range and at pD

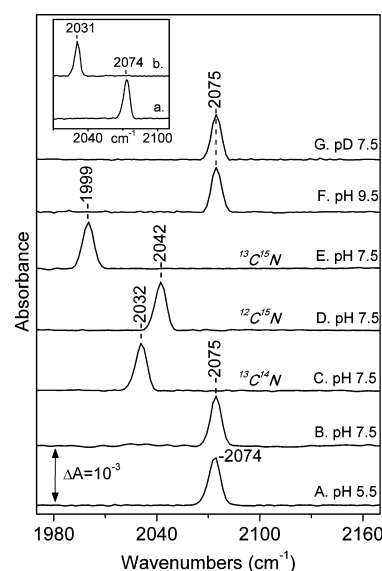


**Figure 3.** FTIR spectra of the reaction of oxidized cytochrome  $ba_3$  with  $^{12}\text{C}^{14}\text{N}$  at pH 5.5 (trace A), pH 7.5 (trace B), pH 9.5 (trace F), and pD 7.5 (trace G) 24 h subsequent to CN $^-$  addition to the oxidized enzyme. The FTIR spectra of the  $ba_3$ - $^{13}\text{C}^{14}\text{N}$  (trace C),  $ba_3$ - $^{12}\text{C}^{15}\text{N}$  (trace D), and  $ba_3$ - $^{13}\text{C}^{15}\text{N}$  (trace E) adducts at pH 7.5 are included. The inset presents the FTIR spectra of the reaction of the fully reduced cytochrome  $ba_3$  with  $^{12}\text{C}^{14}\text{N}$  (trace a) and  $^{13}\text{C}^{14}\text{N}$  (trace b) at pH 7.5.

7.5. Trace A corresponds to the FTIR spectrum of the oxidized  $ba_3$ - $^{12}\text{C}^{14}\text{N}$  reaction at pH 5.5 and displays one vibration at 2074  $\text{cm}^{-1}$  that shifts by 1  $\text{cm}^{-1}$  to 2075  $\text{cm}^{-1}$  at pH 7.5 (trace B), pH 9.5 (trace F) and pD 7.5 (trace G). The 2075  $\text{cm}^{-1}$  mode shifts to 2032  $\text{cm}^{-1}$  in the spectrum of the  $^{13}\text{C}^{14}\text{N}$  adduct (trace C), to 2042  $\text{cm}^{-1}$  in the  $^{12}\text{C}^{15}\text{N}$  adduct (trace D), and to 1999  $\text{cm}^{-1}$  (trace E) in the  $^{13}\text{C}^{15}\text{N}$  adduct. As described previously, the frequency of this mode and its isotopic shifts allow us to assign it to the C–N stretching vibration of the heme  $a_3^{2+}$ -CN $^-$  complex. The inset presents the FTIR spectra of the fully reduced cytochrome  $ba_3$ - $^{12}\text{C}^{14}\text{N}$  (trace a) and  $^{13}\text{C}^{14}\text{N}$  (trace b) adducts at pH 7.5 that presents the  $\nu(\text{C–N})$  of the heme  $a_3^{2+}$ -CN $^-$  adduct at 2074  $\text{cm}^{-1}$ .

Figure 4 displays the light-minus-dark FTIR spectra of the oxidized  $ba_3$ - $^{12}\text{C}^{14}\text{N}$  adducts at pH 5.5 (trace A), pH 7.5 (trace B), pH 9.5 (trace F). The negative mode at 2074  $\text{cm}^{-1}$  (trace A) and at 2075  $\text{cm}^{-1}$  (traces B, F and G) indicate the dissociation of CN $^-$  from heme  $a_3^{2+}$ , and the concomitant appearance of a positive band at 2146  $\text{cm}^{-1}$  is attributed to the formation of a transient Cu $_B^{2+}$ -CN $^-$  complex. The latter mode



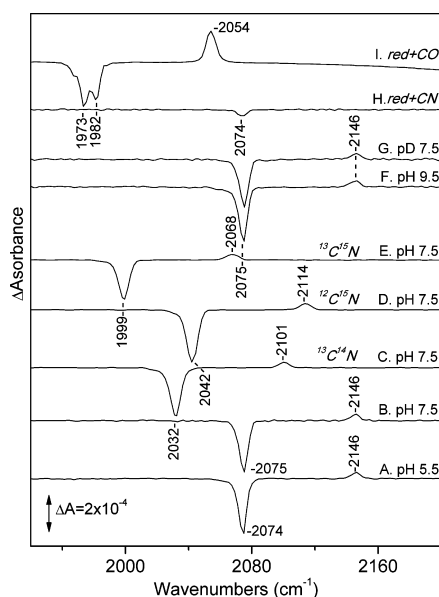


**Figure 4.** Light-minus-dark FTIR difference spectra of the oxidized  $ba_3$ -CN adduct at pH 5.5 (trace A), pH 7.5 (trace B), pH 9.5 (trace F), and pD 7.5 (trace G). The light-minus-dark FTIR difference spectra of the  $ba_3$ - $^{13}C^{14}N$  (trace C),  $ba_3$ - $^{12}C^{15}N$  (trace D), and  $ba_3$ - $^{13}C^{15}N$  (trace E) adducts at pH 7.5 are included. Trace H is the light-minus-dark FTIR difference spectrum of the fully reduced  $ba_3$ - $^{12}C^{14}N$  adduct. Trace I is the light minus-dark-difference FTIR spectrum of the fully reduced cytochrome  $ba_3$ -CO adduct. The photolysis wavelength was 447 nm and the incident power on the sample was 30 mW.

shifts to 2101  $cm^{-1}$  in the  $ba_3$ - $^{13}C^{14}N$  photoproduct (trace C), and to 2114 and 2068  $cm^{-1}$  in the  $ba_3$ - $^{12}C^{15}N$  (trace D) and  $ba_3$ - $^{13}C^{15}N$  (trace E) photoproducts, respectively. The frequency of this vibration indicates that  $Cu_B$  remains oxidized, since the  $\nu(Cu_B^{1+}C-N)$  vibrations have been reported at 2037 and 2093  $cm^{-1}$ .<sup>26</sup> The yield for the photoproduct was  $\sim 30\%$  for the oxidized  $ba_3$ -cyanide adducts. Trace H corresponds to the light-minus-dark FTIR spectrum of the fully reduced  $ba_3$ -CN complex. The small intensity of the negative band at 2074  $cm^{-1}$  (5% relative to the initial spectrum) indicates that the photoproduct is formed at a very low percentage. For comparison, we have included the light-minus-dark FTIR spectrum of the fully reduced  $ba_3$ -CO adduct that demonstrates the transfer of CO from the heme  $a_3^{2+}$  (1973 and 1982  $cm^{-1}$  bands) to  $Cu_B^{1+}$  (2054  $cm^{-1}$ ) upon illumination with 447 nm light.<sup>6</sup>

## DISCUSSION

**The Heme  $a_3^{3+}$ - $C\equiv N$ - $Cu_B^{2+}$ , Heme  $a_3^{2+}$ -CN $^-$ / $Cu_B^{2+}$ , and Heme  $a_3^{2+}$ / $Cu_B^{2+}$ -CN $^-$  Species.** Despite the distinct differences in the ligand binding properties of  $ba_3$  oxidase when compared to the other heme-copper oxidases, the frequency at 2152  $cm^{-1}$  is similar to that observed and assigned to a bridging heme  $Fe^{3+}$ - $C\equiv N$ - $Cu_B^{2+}$  structure in the majority of heme-copper oxidases on the basis of isotope replacement experiments.<sup>24–26,29</sup> In the heme  $a_3^{2+}$ -CN $^-$  complex shown in Figure 3 (traces A, B, F, G) the frequency of the  $\nu(CN)$  mode is invariant between pH 5.5 and 9.5 and unaffected by H/D exchange, consistent with no change in the protonation of groups in close proximity to cyanide under our experimental conditions. The frequency of  $\nu(CN)$  reported here is 16 and 37  $cm^{-1}$  higher than that observed in  $aa_3$  and  $bo_3$  oxidases, respectively.<sup>26,28</sup> The large frequency differences between the

CN isotope-sensitive modes in the reduced CN-bound forms of heme  $a_3$  and heme  $o_3$  indicate that despite the great similarities in the frequencies of the oxidized CN-bridging forms, the Heme  $Fe^{2+}$ -CN $^-$ / $Cu_B^{2+}$  moiety of  $ba_3$  oxidase experiences significant changes compared to its mammalian and *Escherichia coli* counterparts that influence the frequencies of the bound CN $^-$ .

It is well established that the proximal histidine is a good  $\sigma$  and  $\pi$  donor to the heme  $Fe^{2+}$  and the heme is a  $\pi$  acceptor, while cyanide is a weak  $\pi$  acceptor and a good  $\sigma$  donor. Vibrational analysis predicts that weakening of the trans-axial ligand bond is expected to cause a stronger  $\sigma$  donation from the CN $^-$  via a trans effect. Similarly, the weaker  $\pi$  donation from the histidine will tend to weaken the Fe-CN  $d_\pi$  backbonding, leading to an increase of the  $\nu(CN)$ .<sup>19,20,30</sup> Therefore the main factors that contribute to the high frequency of the bound CN in  $ba_3$  oxidase compared to the analogous vibrations in  $aa_3$  and  $bo_3$  oxidases include (i) the interactions of the proximal to the heme  $a_3$  Fe-histidine with the protein environment which essentially affect its basicity and (ii) the electron density withdrawal from the formyl group of heme  $a_3$  and the protonation/deprotonation of the heme  $a_3$  propionates upon ligand binding to the heme  $a_3$  Fe.<sup>19,20,34,35</sup> In addition, these factors can contribute to the electron density of the heme-Fe making it electron poor and thus, susceptible to autoreduction by cyanide.<sup>20</sup> Therefore, the initially formed heme  $Fe^{3+}$ - $C\equiv N$ - $Cu_B^{2+}$  complex, due to the properties of the heme Fe, is converted to heme  $a_3^{2+}$ -CN $^-$  leaving  $Cu_B^{2+}$  as a spectator in the event. The similarity in the frequency of  $\nu(CN)$  in the  $a_3^{2+}$ -CN $^-$ / $Cu_B^{2+}$  species with that observed in the  $a_3^{2+}$ -CN $^-$ / $Cu_B^{1+}$  suggests that the oxidation state of  $Cu_B$  does not influence the strength of the  $a_3^{2+}$ -CN $^-$  and that the effect from the proximal histidine is the same regardless of the way the  $a_3^{2+}$ -CN $^-$  species was formed.

The frequencies of CN $^-$  bound to  $Cu^{1+}$  and  $Cu^{2+}$  in heme-copper oxidases, in the Cu-containing enzyme nitrite reductase, and in model Cu compounds are summarized in Table 1.<sup>26,36,37</sup>

**Table 1. C–N Stretching Frequencies ( $cm^{-1}$ ) for  $Cu^{1+}$ -CN and  $Cu^{2+}$ -CN Complexes**

	$^{12}C^{14}N$	$^{12}C^{15}N$	$^{13}C^{14}N$	$^{13}C^{15}N$
C–N stretching frequencies for $Cu^{1+}$ -CN complexes				
Cytochrome $aa_3$ (bovine) <sup>a</sup>	2093	2060	2049	2016
	2037	2006	1995	1964
Nitrite reductase ( <i>Alcaligenes faecalis</i> ) <sup>b</sup>	2065			
(Et <sub>4</sub> N)[Cu(HB(Me <sub>2</sub> pz) <sub>3</sub> (CN))] <sup>c</sup>	2077			
C–N stretching frequencies for $Cu^{2+}$ -CN complexes				
Cu/Zn superoxide dismutase <sup>d</sup>	2137			
[Cu(Npy <sub>3</sub> )(CN)] <sup>+c</sup>	2142			
Cytochrome $ba_3$ ( <i>T. thermophilus</i> ) <sup>e</sup>	2146	2114	2101	2068

<sup>a</sup>Reference 26. <sup>b</sup>Pinakoulaki et al., unpublished results. <sup>c</sup>Reference 36. <sup>d</sup>Reference 37. <sup>e</sup>This work.

A close inspection of the  $\nu(CN)$  frequencies suggests that the frequency we observe at 2146  $cm^{-1}$  is due to the formation of a  $Cu_B^{2+}$ -CN $^-$  transient species. The observed frequencies of  $Cu^{1+}$ -CN $^-$  in heme-copper oxidases, nitrite reductase, and model compounds vary from 2037 to 2093  $cm^{-1}$ .<sup>26,36</sup> Infrared spectra of solid CuCN have revealed the  $\nu(CN)$  at 2170  $cm^{-1}$ .<sup>37</sup> Early studies have shown that cyanide which binds via its carbon end to Cu is sensitive to the other ligands in the complex and is, thus, a powerful probe of Cu coordination. The

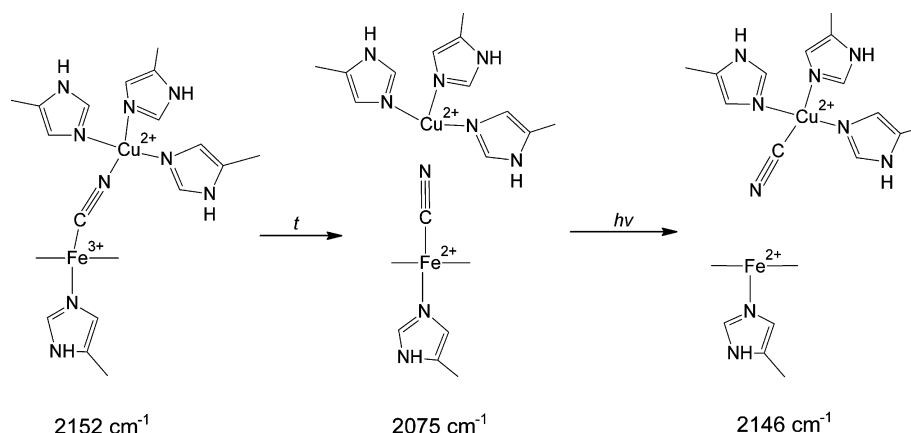


**Figure 5.** Schematic illustration of the structures of CN-bound forms of *ba*<sub>3</sub> oxidase and the photolysis product.

relationship between  $\nu(\text{CN})$  and the coordination environment is determined by the mode of cyanide binding to Cu. The Cu–C bond is formed by the donation of two electrons which are localized on the C atom. As  $\text{CN}^-$  is a good  $\sigma$ -donor and a poor  $\pi$ -acceptor, the two electrons which are weakly antibonding in the free ligand become bonding upon coordination to Cu. Consequently, the frequency of  $\text{CN}^-$  is expected to increase upon binding to  $\text{Cu}_\text{B}^{2+}$ . The greater the basicity or  $\sigma$ -donor of the other ligands coordinated to  $\text{Cu}_\text{B}$ , the more the frequency will be increased over that of the free cyanide.<sup>36</sup> Indeed the frequency of the bound  $\text{CN}^-$  to  $\text{Cu}^{2+}$  is at  $2146\text{ cm}^{-1}$  which is  $66\text{ cm}^{-1}$  higher than that of free  $\text{CN}^-$ . The frequency we have observed is similar to those observed in the Cu/Zn superoxide dismutase at  $2137\text{ cm}^{-1}$  and in  $[\text{Cu}(\text{Npyr}_3)(\text{CN})]$  complex at  $2142\text{ cm}^{-1}$ .<sup>36,37</sup> The latter complex mimics the cyanide interaction with Cu in heme-copper oxidases.

We can derive structural information for the  $\text{Cu}_\text{B}^{2+}\text{--N}(\text{His})$  ligands from the  $\nu(\text{CN})$  frequency of the  $\text{Cu}_\text{B}^{2+}\text{--CN}^-$  complex as we did from the  $\nu(\text{CO})$  frequency of the  $\text{Cu}_\text{B}^{1+}\text{--CO}$  complex. If a change in the protonation state of one of the His ligands occurred, it would influence its basicity and would thus affect the  $\nu(\text{CN})$  frequency. However, the insensitivity of the  $\nu(\text{CN})$  of the  $\text{Cu}_\text{B}^{2+}\text{--CN}^-$  complex to  $\text{H}_2\text{O}/\text{D}_2\text{O}$  exchange and to pH 5.5–9.5 range indicate that the  $\text{Cu}_\text{B}^{2+}\text{--His}$  environment is very rigid and not subject to conformational transitions that are associated with protonation/deprotonation events of the  $\text{Cu}_\text{B}^{2+}$  His ligands. Similar conclusions were made in the case of the  $\text{Cu}_\text{B}^{1+}\text{--CO}$  complex.<sup>6,7</sup> Therefore, the  $\text{Cu}_\text{B}$  His environment is inflexible in both oxidation states of the metal.

**Ligand Transfer and Bond Formation.** The dynamics of ligand binding and escape in heme-copper oxidases provides information on the intrinsic reactivity of the active site and how the reactivity and the migration pathway of the ligand are controlled by the protein. Observation of the motion of ligands such as CO, O<sub>2</sub>, NO, and  $\text{CN}^-$  within the heme-copper oxidases is facilitated by photodissociation. After dissociation from the heme at physiological temperatures, ligands either rebound geminantly from within the distal heme pocket or bind transiently to the nearby  $\text{Cu}_\text{B}$  and subsequently rebound to the heme Fe. The extent of geminate recombination depends on the intrinsic reactivity of the ligand with the heme Fe and its ability to bind to  $\text{Cu}_\text{B}$  or diffuse away from the binuclear heme Fe– $\text{Cu}_\text{B}$  site. The role of  $\text{Cu}_\text{B}$  has been revealed in the case of CO binding to *ba*<sub>3</sub> oxidase.<sup>6–9</sup> The detailed thermodynamics and kinetics data of CO binding/rebinding have been compared and there is evident chemical difference between

*ba*<sub>3</sub> and the other heme-copper oxidases.<sup>4,5</sup> In an attempt to identify the ligand binding entry and the product escape in heme-copper oxidases, the primary ligand intermediate in cytochrome *ba*<sub>3</sub> from *T. thermophilus* has been recently identified.<sup>8</sup> In this study, the process of ligand docking that represents the ligand escape pathway along with the ligand binding pathway was used to describe the intermediate states occupied during conformational transitions in *ba*<sub>3</sub> oxidase. The “docked” CO was observed by its frequency at  $2131\text{ cm}^{-1}$  found to be located near the ring A of heme *a*<sub>3</sub> propionate that is 4.2 Å away from the heme *a*<sub>3</sub> Fe.<sup>8</sup>

The room temperature FTIR photolysis spectra shown in Figure 4 (traces A–G) represent the difference between the mixed valence  $\text{a}_3^{2+}/\text{Cu}_\text{B}^{2+}$  binuclear center with  $\text{CN}^-$  bound to the heme and the mixed valence  $\text{a}_3^{2+}/\text{Cu}_\text{B}^{2+}$  with the  $\text{CN}^-$  bound to  $\text{Cu}_\text{B}^{2+}$ . This demonstrates the absence of activation barriers to  $\text{CN}^-$  transfer from heme  $\text{a}_3^{2+}$  to  $\text{Cu}_\text{B}^{2+}$ . The corresponding FTIR photolysis spectrum of the fully reduced *ba*<sub>3</sub>–CN adduct (trace H) represents the difference between the fully reduced enzyme with CN-bound to the heme Fe and the reduced enzyme with  $\text{CN}^-$  not bound to the enzyme. Therefore, the transfer of cyanide from one metal to the other (the metals are located about 4–5 Å apart) is observed only for the mixed valence binuclear center. The photolysis product of the heme  $\text{a}_3^{2+}\text{--CN}^-/\text{Cu}_\text{B}^{2+}$  differs from the corresponding heme  $\text{a}_3^{2+}\text{--CN}^-/\text{Cu}_\text{B}^{1+}$  product, and the recombination of cyanide to the heme is slowed substantially in the first case. The affinity of  $\text{Cu}_\text{B}^{2+}$  versus  $\text{Cu}_\text{B}^{1+}$  for cyanide may be proposed as a rate-limiting step to geminate recombination. The current work shows for the first time that the transient  $\text{Cu}_\text{B}^{2+}\text{--CN}^-$  adduct of *ba*<sub>3</sub> oxidase is formed at a substantial level of occupancy, is long-lived, and is spectroscopically observable. We do not have any evidence for the photochemical properties of the  $\text{Cu}_\text{B}^{2+}\text{--CN}^-$  complex, and thus, we presume that is not photolabile by 447 nm excitation. Figure 5 shows a schematic illustration of the structures of CN-bound forms and the photolysis product. The photochemical activity that we observed for the cyanide complex is surprising and was not expected *a priori*. The photochemical activities of  $\text{Cu}^{2+}$ - and  $\text{Cu}^{1+}\text{--CN}^-$  bound complexes have not been explored extensively. Quantum yields, wavelength dependencies, and the excited states involved in these photochemical activities have yet to be characterized.

We have recently reported the reaction of both oxidized and reduced *ba*<sub>3</sub> with NO.<sup>10,12</sup> On the basis of our observations we proposed a reaction scheme for the initial binding of two NO

molecules to the oxidized heme  $a_3$ -Cu<sub>B</sub> binuclear center.<sup>12</sup> Since the formation of the N–N bond required the addition of an electron we proposed that the hyponitrite species is formed subsequent to the formation of a transient heme  $a_3^{3+}$ -NO species and the addition of the second NO molecule to Cu<sub>B</sub>. Given that upon addition of NO to the oxidized enzyme the heme  $a_3$  is in the ferric form, then Cu<sub>B</sub> must be reduced upon the addition of NO producing Cu<sub>B</sub><sup>1+</sup> and NO<sub>2</sub><sup>−</sup>. This is not the case in the reaction of oxidized  $ba_3$  oxidase with CN<sup>−</sup>. The binuclear center binds only one CN<sup>−</sup> molecule and Cu<sub>B</sub> remains oxidized upon transient binding of CN<sup>−</sup> leaving the binuclear center in the unique mixed valence form of heme  $a_3^{2+}$ /Cu<sub>B</sub><sup>2+</sup>–CN<sup>−</sup>.

## CONCLUSIONS

This work reports evidence for ligand transfer in a unique mixed valence binuclear center in heme-copper oxidases. The experiments presented here represent the initial efforts to understand the complex interplay between the autoreduction of the heme Fe and ligand transfer in the binuclear center of cytochrome *c* oxidase leaving the binuclear center in a mixed valence form. Previous experiments have failed to report that prior to the formation of the heme  $a_3^{2+}$ -CN<sup>−</sup>, the bridging cyanide complex was formed in  $ba_3$  oxidase.<sup>18</sup> The observation of the heme  $a_3^{3+}$ -CN-Cu<sub>B</sub><sup>2+</sup>, the heme  $a_3^{2+}$ -CN<sup>−</sup>/Cu<sub>B</sub><sup>2+</sup>, the heme  $a_3^{2+}$ -CN<sup>−</sup>/Cu<sub>B</sub><sup>1+</sup> and the transient heme  $a_3^{2+}$ /Cu<sub>B</sub><sup>+2</sup>-CN<sup>−</sup> species at room temperature forms a foundation for understanding of the Cu<sub>B</sub> environment and the molecular relaxation pathway of photodissociation reactions in  $ba_3$  oxidase. To uncover the relaxation pathway it will be necessary to study the transient species by different techniques and to derive information from their time evolution at physiological temperatures. Indeed, measurements at the optimal growth temperature of the bacterium of 70 °C are lacking in the literature. Such studies will lead to an advanced understanding of the dynamic processes and the reaction pathways that occur in heme-copper oxidases, and elucidate the role of Cu<sub>B</sub> as the obligatory site for the exit and entry of ligands to the reduced, oxidized, and mixed valence binuclear center.

## AUTHOR INFORMATION

### Corresponding Author

\*E-mail: effiep@ucy.ac.cy.

### Notes

The authors declare no competing financial interest.

## ACKNOWLEDGMENTS

This work was funded by the European Regional Development Fund and the Republic of Cyprus through the Research Promotion Foundation (Infrastructure Project ANAVATHMI-SI/PAGIO/0308/14) to E.P., and by the Science Foundation Ireland BICF865 to T.S. The authors thank Mrs. Maria Achilleos for preliminary measurements.

## REFERENCES

- (1) Than, M. E.; Soulimane, T. *Handbook of Metalloproteins*; Wiley: New York, 2001; pp 363–378.
- (2) Soulimane, T.; Buse, G.; Bourenkov, G. P.; Bartunik, H. D.; Huber, R.; Than, M. E. *EMBO J.* **2000**, *19*, 1766–1776.
- (3) Giuffrè, A.; Stubauer, G.; Sart, P.; Brunori, M.; Zumft, W. G.; Buse, G.; Soulimane, T. *Proc. Natl. Acad. Sci. U.S.A.* **1999**, *96*, 14718–14723.
- (4) Goldbeck, R. A.; Einarsdóttir, O.; Dawes, T. D.; O'Connor, D. B.; Surerus, K. K.; Fee, J. A.; Kliger, D. S. *Biochemistry* **1992**, *31*, 9376–9387.
- (5) Giuffrè, A.; Forte, E.; Antonini, G.; D'Itri, E.; Brunori, M.; Soulimane, T.; Buse, G. *Biochemistry* **1999**, *38*, 1057–1065.
- (6) Koutsoupakis, K.; Stavakis, S.; Pinakoulaki, E.; Soulimane, T.; Varotsis, C. *J. Biol. Chem.* **2002**, *277*, 32860–32866.
- (7) Koutsoupakis, K.; Stavakis, S.; Soulimane, T.; Varotsis, C. *J. Biol. Chem.* **2003**, *278*, 14893–14896.
- (8) Koutsoupakis, C.; Soulimane, T.; Varotsis, C. *J. Am. Chem. Soc.* **2003**, *125*, 14728–14732.
- (9) Koutsoupakis, C.; Soulimane, T.; Varotsis, C. *Biophys. J.* **2004**, *86*, 2438–2444.
- (10) Pinakoulaki, E.; Ohta, T.; Soulimane, T.; Kitagawa, T.; Varotsis, C. *J. Am. Chem. Soc.* **2005**, *127*, 15161–15167.
- (11) Ohta, T.; Kitagawa, T.; Varotsis, C. *Inorg. Chem.* **2006**, *45*, 3187–3190.
- (12) Varotsis, C.; Ohta, T.; Kitagawa, T.; Soulimane, T.; Pinakoulaki, E. *Angew. Chem. Int. Ed.* **2007**, *46*, 2210–2214.
- (13) Pinakoulaki, E.; Varotsis, C. *J. Inorg. Biochem.* **2008**, *102*, 1277–1287.
- (14) Porrini, M.; Daskalakis, V.; Farantos, S.; Varotsis, C. *J. Phys. Chem B* **2009**, *112*, 12129–12135.
- (15) Koutsoupakis, C.; Kolaj-Robin, O.; Soulimane, T.; Varotsis, C. *J. Biol. Chem.* **2011**, *285*, 30600–30605.
- (16) Hayashi, T.; Lin, I. J.; Chen, Y.; Fee, J. A.; Moenne-Loccoz, P. *J. Am. Chem. Soc.* **2007**, *129*, 14952–14958.
- (17) Pilet, E.; Nitschke, W.; Rappaport, F.; Soulimane, T.; Lambry, J. C.; Liebl, U.; Vos, M. H. *Biochemistry* **2004**, *43*, 14118–14127.
- (18) Surerus, K. K.; Oertling, W. A.; Fan, C.; Gurbiel, R. J.; Einarsdóttir, O.; Antholine, W. E.; Dyer, R. B.; Hoffman, B. M.; Woodruff, W. H.; Fee, J. A. *Proc. Natl. Acad. Sci. U.S.A.* **1992**, *89*, 3195–3199.
- (19) Kim, Y.; Babcock, G. T.; Surerus, K. K.; Fee, J. A.; Dyer, R. B.; Woodruff, W. H.; Oertling, W. A. *Biospectroscopy* **1998**, *4*, 1–15.
- (20) Oertling, W. A.; Surerus, K. K.; Einarsdóttir, O.; Fee, J. A.; Dyer, R. B.; Woodruff, W. H. *Biochemistry* **1994**, *33*, 3128–3141.
- (21) Luna, V. M.; Chen, Y.; Fee, J. A.; Stout, C. D. *Biochemistry* **2008**, *33*, 4657–4665.
- (22) Kalinovich, A. V.; Azarkina, N. V.; Vygodina, T. V.; Soulimane, T.; Konstantinov, A. A. *Biochemistry (Moscow)* **2010**, *75*, 342–352.
- (23) Nicholls, P.; Soulimane, T. *Biochem. Biophys. Acta* **2004**, *1655*, 381–387.
- (24) Yoshikawa, S.; Caughey, W. S. *J. Biol. Chem.* **1990**, *265*, 7945–7958.
- (25) Yoshikawa, S.; Mochizuki, M.; Zhao, X.-J.; Caughey, W. S. *J. Biol. Chem.* **1995**, *270*, 4270–4279.
- (26) Tsubaki, M.; Yoshikawa, S. *Biochemistry* **1993**, *32*, 164–173.
- (27) Hirota, S.; Ogura, T.; Shinzawa-Itoh, K.; Yoshikawa, S.; Kitagawa, T. *J. Phys. Chem.* **1996**, *100*, 15274–15279.
- (28) Tsubaki, M.; Mogi, T.; Hori, H.; Sato-Watanabe, M.; Anraku, Y. *J. Biol. Chem.* **1996**, *271*, 4017–4022.
- (29) Pinakoulaki, E.; Vamvouka, M.; Varotsis, C. *J. Phys. Chem. B* **2003**, *107*, 9865–9868.
- (30) Pinakoulaki, E.; Vamvouka, M.; Varotsis, C. *Inorg. Chem.* **2004**, *43*, 4907–4910.
- (31) Rich, P. R.; Breton, J. *Biochemistry* **2001**, *40*, 6441–6449.
- (32) Parul, D.; Palmer, G.; Fabian, M. *J. Biol. Chem.* **2010**, *285*, 4536–4543.
- (33) Butler, C.; Forte, E.; Scandurra, F. M.; Arese, M.; Giuffrè, A.; Greenwood, C.; Sarti, P. *Biochem. Biophys. Res. Commun.* **2002**, *296*, 1272–1278.
- (34) Xu, C.; Ibrahim, M.; Spiro, T. G. *Biochemistry* **2008**, *47*, 2379–2387.
- (35) Pavlou, A.; Soulimane, T.; Pinakoulaki, E. *J. Phys. Chem. B* **2011**, *115*, 11455–11461.
- (36) Lim, B. S.; Holm, R. H. *Inorg. Chem.* **1998**, *37*, 4898–4908.
- (37) Han, J.; Blackburn, N. J.; Loehr, T. M. *Inorg. Chem.* **1992**, *31*, 3223–3229.